Article

Aggregation-Induced Emission of Water-Soluble Tetraphenylethene Derivatives at Polarized Liquid|Liquid Interfaces

Makoto Nabara, Sho Yamamoto, Yoshio Nishiyama, and Hirohisa Nagatani

Langmuir, **Just Accepted Manuscript** • DOI: 10.1021/acs.langmuir.0c01962 • Publication Date (Web): 07 Aug 2020

Aggregation-Induced Emission of Water-Soluble Tetraphenylethene Derivatives at Polarized Liquid|Liquid Interfaces

Makoto Nabara,[†] *Sho Yamamoto,*[†] *Yoshio Nishiyama,*[†,‡] *and Hirohisa Nagatani*[*,†,‡]

[†] Division of Material Chemistry, Graduate School of Natural Science and Technology, Kanazawa University, Kakuma, Kanazawa 920-1192, Japan

[‡] Faculty of Chemistry, Institute of Science and Engineering, Kanazawa University, Kakuma, Kanazawa 920-1192, Japan

*To whom correspondence should be addressed: H. Nagatani

Tel: +81 76 264 5694

E-mail: nagatani@se.kanazawa-u.ac.jp

ABSTRACT

Aggregation-induced emission (AIE) behavior of water-soluble tetraphenylethene (TPE) derivatives bearing carboxy and sulfo groups was studied at polarized liquid|liquid interfaces. The aggregation behavior of TPE derivatives in solution and at the water|1,2-dichloroethane (DCE) interface was highly dependent on their ionizable functional groups. Spectroelectrochemical analysis elucidated that the TPE derivatives were transferred across the interface accompanied by the adsorption process at the interface. The ion transfer and interfacial AIE features of TPEs responded reversibly to the externally applied potential, indicating no rigid crystalline structure formation in the interfacial region. The red-shift measured in intense interfacial emission spectra demonstrated that the carboxylate derivatives formed their J-aggregates specifically at the polarized water|DCE interface, while the aggregation processes with distinguishable emission properties took place in both interfacial region and organic solution in the sulfonate derivative system. The AIE features were also investigated at a glycerophospholipid-adsorbed interface as a model of biomembrane surface. The aggregation process of TPE derivatives was significantly modified through the interaction with phospholipid layers which stimulate the interfacial AIE process of tetra-anionic TPEs.

KEYWORDS: Aggregation-induced emission (AIE); Interface between two immiscible electrolyte solutions (ITIES); Tetraphenylethene (TPE); Polarization-modulation total internal reflection fluorescence (PM-TIRF); Potential-modulated fluorescence (PMF)

INTRODUCTION

A variety of organic luminescent molecules have been developed as spectrophotometric reagents for trace detection, bioimaging probes, sensitizers for photo-energy conversion, hosts/dopants for organic light-emitting devices and so on. The conventional aromatic fluorescent dyes with π-conjugated system show a concentration quenching effect often referred as aggregation-caused quenching (ACQ) with π-π stacking interaction.[1-3] ACQ of fluorescent dyes impedes their effective applications on surfaces and at interfaces, where an enrichment of dye molecules with a certain surface-activity takes place spontaneously. Recent developments of aggregation-induced emission (AIE) system demonstrate promising applications in functional materials, optoelectronic and biomedical purposes.[4-7] Tang and his coworkers have reported effective AIE features of a series of propeller shape compounds such as hexaphenylsiole (HPS) and tetraphenylethene (TPE) derivatives which undergo nonradiative relaxation in their monomer forms.[8-10] These AIE luminogens (AIEgens) exhibit emissive features in the aggregated state because of the restriction of intramolecular motion (RIM), including rotation and vibration of the multiple phenyl groups.[11, 12]

An interface between two immiscible electrolyte solutions (ITIES) has been utilized as a two-dimensional reaction field for the formation of nanomaterials and 2D supramolecular architectures based on specific adsorption and phase transfer of reactants,[13-16] and as a model of biomembrane surface to evaluate mass transport and pharmacokinetics in biomimetic systems.[17-19] Various dye species and nanomaterials show self-aggregation/assemble features at polarized liquid|liquid interfaces, where the extent of aggregation of charged species can reversibly be controlled as a function of externally applied potential.[20-24] The potential-driven aggregation accompanied by a colorimetric response is favorable for biomembrane imaging with a membrane potential-

sensitivity. The membrane potential of the living cell plays a crucial role in physiological processes, including nerve impulse transmission and mass-transfer process of charged species moving into or out of the cell. A variety of voltage-sensitive dyes have been developed and used as a molecular probe in biochemical applications.[25-30] Those dyes, however, exhibit emission properties mostly in the ACQ mechanism, which is not ideal to evaluate membrane potential with high-sensitivity in fluorescence imaging. Some AIEgens demonstrate their abilities as a membrane potential indicator for organic tissues as well as a photosensitizer for cancer phototherapy with selective staining of specific cells.[31-35] The adsorption and aggregation behavior of AIEgen at liquid|liquid interfaces, especially at a phospholipid-adsorbed biomimetic interface, under electrochemical control are thus important to elucidate their membrane potential-sensitive mechanism. It has been reported that surface-active AIEgens show the adsorption-promoted aggregation and emission induced by efficient lateral interaction of adsorbed molecules at liquid phase boundaries and on solid surfaces,[36-38] but no detailed analysis of the AIE effect at the liquid|liquid interface.

In this study, the interfacial aggregation and AIE features of anionic TPE derivatives were investigated at the water|1,2-dichloroethane (DCE) interface by surface-sensitive spectroelectrochemical techniques, i.e., potential-modulated fluorescence (PMF) spectroscopy and polarization-modulation total internal reflection (PM-TIRF) spectroscopy.[39-41] The analysis of ac-modulated optical signals in the potential- and light polarization-modulation spectroscopies effectively improves the selectivity to the interfacial optical signals in comparison to the conventional differential voltfluorometry and TIRF spectroscopy.[42-44] PMF spectroscopy is a powerful tool to elucidate a potential-driven interfacial process of charged species, while PM-TIRF spectroscopy allowed us to characterize the adsorption species oriented at the interface. The aggregation behavior of TPE derivatives in solution and at ITIES were highly dependent on their

ionizable functional groups, and their interfacial AIE behavior responded to the externally applied potential. The AIE features of TPE derivatives were also examined at a biomimetic phospholipid-adsorbed interface.

EXPERIMENTAL SECTION

Reagents. Tetrakis(4-sulfophenyl)ethene (H_4TPETS) and its lithium salt were synthesized from tetraphenylethene (TPE) (Sigma-Aldrich, 98%) according to a literature method.[45, 46] TPE was stirred in conc. H_2SO_4 at 388 K for 4 hrs and then the resulting H_4TPETS was obtained as precipitate by adding the reaction mixture dropwise into an ice-cooled ethyl acetate. The precipitate was washed with ethyl acetate and dried in vacuum at 353 K. The H_4TPETS recrystallized from methanol-ethyl acetate mixture was dissolved in 0.10 mol dm^{-3} LiOH aqueous solution and the evaporation of water left a readily water-soluble TPETS lithium salt (cf. ^{1}H NMR data in **Supporting Information: S1**). Tetrakis(4-carboxyphenyl)ethene (H_4TPETC) and 1,2-di(4-carboxyphenyl)-1,2-diphenylethene (H_2TPEDC) were purchased from Strem Chemicals (99%) and Sigma-Aldrich (98%), respectively and used without further purification. The aqueous solutions were prepared with purified water by a Milli-Q system (Millipore, Direct-Q3UV). All other reagents were of the highest grade available. The absorption and emission spectra of the TPE derivatives in solution were measured by a JASCO V-750 UV-vis spectrophotometer and a JASCO FP-8300 spectrofluorometer, respectively. The pH condition of the aqueous solution was adjusted by the addition of an adequate amount of H_2SO_4 (pH ≤ 3.2) or 2.0×10^{-3} mol dm^{-3} buffers, i.e. (pH 5.6) CH_3COOH/CH_3COOLi, (pH 7) LiH2PO4/LiOH, and (8.8 ≤ pH) H3BO3/LiOH. The composition of the electrochemical cells is illustrated in **Figure 1**. The purified water and 1,2-

dichloroethane (DCE) (Nacalai Tesque, HPLC grade, ≥ 99.7%) as an organic solvent were saturated with each other and used for solution preparation. The supporting electrolytes were 1.0×10^{-2} mol dm^{-3} Li_2SO_4 for the aqueous phase and 5.0×10^{-3} mol dm^{-3} bis(triphenylphosphoranylidene)ammonium tetrakis(pentafluorophenyl)borate (BTPPATPFB) for the organic phase, respectively. BTPPATPFB was prepared by metathesis of bis(triphenylphosphoranylidene)ammonium chloride (BTPPACl) (Aldrich, 97%) and lithium tetrakis(pentafluorophenyl)borate ethyl ether complex (TCI) in a 4:1 mixture of methanol and water, followed by recrystallization from acetone. A neutral glycerophospholipid, 1,2-dimyristoyl-snglycero-3-phosphocholine (DMPC) (TCI, ≥ 97%), was added to the organic phase at 2.0×10^{-5} mol dm^{-3} for the biomimetic water|DCE interface.

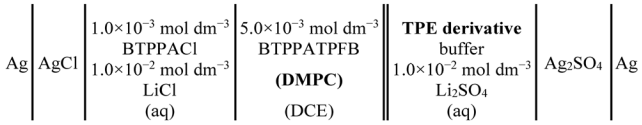

Figure 1. Composition of the electrochemical cell.

Apparatus. Ion transfer voltammetry at the water|DCE interface was performed in a four-electrode spectroelectrochemical cell with the interfacial area of 0.50 cm^2.[47] Cyclic and ac voltammograms were measured by a four-electrode potentiostat (Hokuto Denko, HA-1010mM1A) with a lock-in amplifier (NF, LI5640). The Galvani potential difference ($\Delta_o^w\phi \equiv \phi^w - \phi^o$) was estimated by taking the formal transfer potential ($\Delta_o^w\phi^{o\prime}$) of tetramethylammonium ion as 0.160 V.[48] In the spectroelectrochemical measurements, the water|DCE interface was illuminated in total internal reflection (TIR) with the angle of incidence (ψ) at ca. 75° by a cw laser diode at 376 nm (Coherent, OBIS 375LX-50). The laser power was attenuated to 10 mW to avoid photobleaching of sample solutions. A Fresnel rhomb half-wave plate (Sigma Koki, FRH-102) was used to select

the linear polarization of the fundamental excitation beam. The fluorescence signal from the interfacial region was detected perpendicularly to the interface by an optical fiber and a monochromator equipped with a photomultiplier tube (Shimadzu, SPG-120S). The absorption and fluorescence spectra in solution were measured by a Jasco V-750 UV-vis spectrophotometer and a Jasco FP-8300 spectrofluorometer, respectively. All experiments were carried out in a thermostated room at 298±2 K.

PMF Analysis. The PMF study was carried out by analyzing the fluorescence signal from the interfacial region as a function of ac potential modulation. The amplitude of the ac potential modulation ($\Delta_o^w \phi_{ac}$) was 20 mV at 1 Hz and the linear sweep rate of $\Delta_o^w \phi_{dc}$ was 5 mV s^{-1} in negative sweep.

$$\Delta_o^w \phi = \Delta_o^w \phi_{dc} + \Delta_o^w \phi_{ac} \exp(i\omega t) \quad (1)$$

where i is an imaginary number and ω is the angular frequency. The real (ΔF_{re}) and imaginary (ΔF_{im}) components of PMF signals were analyzed by a digital lock-in amplifier (NF LI5640). The PMF signals arise only from the polarized interfacial region and unmodulated dc fluorescence signals from the bulk solution phase is negligible. The phase shift of PMF signal provides us to elucidate the charge transfer mechanism including ion transfer and adsorption at either side of the interface. Further details of the analytical procedure are described elsewhere.[39]

PM-TIRF Analysis. The linear light polarization of an excitation beam was modulated at 13 Hz between p- and s-polarizations (i.e. parallel and perpendicular to the plane of incidence) by a half-wave liquid crystal retarder (LCR) thermostated at 318 K (Thorlabs, LCC1111T-A, LCC25/TC200). The polarization modulation efficiency of LCR was estimated as P_m = 0.85 at 376 nm.[40, 41] The PM-TIRF signal ($\Delta F^{p\text{-}s}$) in the case of $P_m \neq 1$ value is expressed by

$$\Delta F^{p\text{-}s} = F_m^p - F_m^s = (2P_m - 1)(F^p - F^s) \quad (2)$$

where F_m^p and F_m^s are the modulated fluorescence intensities measured with p- and s-polarized excitation modes, F^p and F^s are the fluorescence intensities arisen from the species oriented at the interface under p- and s-polarized excitations. The modulated fluorescence signal from the interfacial region was analyzed by a digital lock-in amplifier (NF, LI5640) as a function of periodic polarization modulation of the incident beam. The PM-TIRF spectrum was measured at a fixed potential and the potential dependence of ΔF^{p-s} was recorded at 2 mV s^{-1}.

RESULS AND DISCUSSION

AIE Activity of Water-Soluble TPE Derivatives in Solution. The fluorescence titration experiments of TPE derivatives in aqueous solution were performed in order to investigate their fundamental AIE features. Their solubilities are drastically decreased under acidic conditions and some precipitates were formed as a result of the charge neutralization through the protonation of carboxylates. The emission intensities measured in the TPETC and TPEDC systems were enhanced, respectively, at pH < 6 and pH < 4.5, indicating AIE activity of protonated species in acidic aqueous solutions (**Figure 2**). In addition, the progressive red shifts of absorption and emission bands are indicative of the formation of emissive aggregates of H_4TPETC and H_2TPEDC (**Supporting Information: S2**). In alkaline aqueous solution, the anionic forms of $TPETC^{4-}$ and $TPEDC^{2-}$, indicated no emissive properties. $TPETS^{4-}$ with highly acidic sulfo groups is unprotonated within the examined pH conditions and the intermolecular electrostatic repulsion prevents the formation of self-aggregates. Accordingly, the fluorescence intensity observed for the transparent solution of $TPETS^{4-}$ was negligibly small at 1 < pH < 9, demonstrating that TPETS is substantially AIE-inactive in aqueous solution.

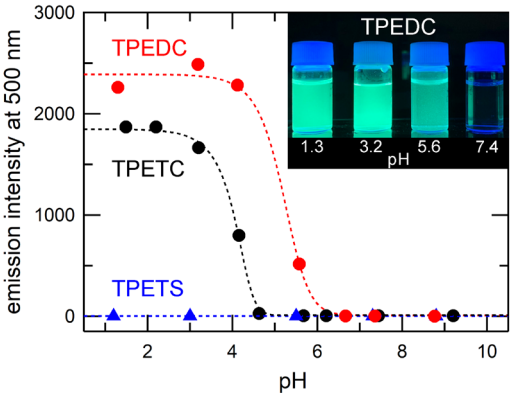

Figure 2. pH dependences of the emission intensity at 500 nm of TPE derivatives in aqueous solution. The red, black, and blue symbols depict TPEDC, TPETC, and TPETS, respectively. The excitation wavelength was 376 nm and the concentration of the TPE derivatives was 2.0×10^{-5} mol dm^{-3}. **Inset**: Typical fluorescence image of TPEDC in aqueous solution under UV irradiation (365 nm).

The self-aggregation behavior of ionic species is generally influenced by solvent properties and the binary mixture system was employed to evaluate solvent effects on AIE features of anionic TPEs. A low polarity solvent, THF is miscible with water, thus the solvent effects arising from hydration-solvation, polarity and other physicochemical properties can be adjusted by a mixing volume ratio of water to THF. For instance, the relative permittivity (ε_r) of water-THF mixture is approximately proportional to the volume fraction of water (f_w / vol%) between those of water ($\varepsilon_{r,w}$ = 78.5) and THF ($\varepsilon_{r,THF}$ = 7.6).[49] The water-THF mixtures with various water fractions were prepared by adding THF to the aqueous solution of TPE derivatives buffered at given pHs (**Supporting Information: S3**). All the examined TPE derivatives exist as nonemissive anionic monomer forms in alkaline aqueous solution (f_w = 100 vol%), whereas the emission intensities for tetraanionic TPE derivatives, TPETC^{4-} and TPETS^{4-}, were drastically increased in low water fraction ($f_w \leq 5$ vol%). These results coincide with previous reports for TPETS in the water-organic solvent mixture systems where the AIE-activity of TPETS with blue-shifted emission in water-THF mixtures is correlated with the self-assembly of nanostructured aggregates.[45] Bhosale and his

co-workers reported rod-like nanostructures at $f_w \leq 5$ vol% but the morphology of resultant emissive aggregates highly depends on the experimental conditions.[46] In contrast, the fluorescence from noncharged acid forms, H_4TPETC and H_2TPEDC, with AIE activity at pH 3 was totally quenched at $f_w < 80$ vol%. These neutral species were readily soluble and nonemissive in THF. The results obtained in the homogeneous solution system demonstrate that the charged and neutral species of the water-soluble TPE derivatives tend to form AIE-active self-aggregates, respectively, in low and high polarity media.

Ion Transfer Across the Water|DCE Interface. The ion transfer voltammograms of $TPEDC^{2-}$ and $TPETC^{4-}$ were measured under alkaline conditions since their protonated species affect the voltammetric response under acidic conditions, while those of $TPETS^{4-}$ were obtained at pH 7.0. The ion transfer responses of $TPEDC^{2-}$ and $TPETC^{4-}$ were observed close to the negative edge of the polarizable potential window, i.e., $\Delta_o^w\phi^{o'}_{TPEDC^{2-}} = -0.30$ V and $\Delta_o^w\phi^{o'}_{TPETC^{4-}} = -0.41$ V (**Figures 3a** and **3b**). $TPEDC^{2-}$ exhibited well-defined quasi-reversible voltammetric responses for dianion with the peak separation of ca.30 mV and the diffusion coefficient in water was estimated as $D^w_{TPEDC^{2-}} = 2.2\times10^{-6}$ cm^2 s^{-1}. Those parameters could not be obtained quantitatively for $TPETC^{4-}$ owing to a significant overlap with the supporting electrolyte transfer. $TPETS^{4-}$ exhibited complicate voltammetric waves at $\Delta_o^w\phi^{o'}_{TPETS^{4-}} = -0.33$ V, where the negative current peak in CVs for the transfer of $TPETS^{4-}$ from water to DCE was accompanied by a post-transfer response corresponding to a sharp admittance peak at −0.39 V (**Figure 3**c). These voltammetric responses could be related to the additional interfacial process of $TPETS^{4-}$. On the other hand, the positive transfer current due to the back transfer to water was obtained as a well-defined diffusion-limited regime. In comparison with the base electrolyte system, the admittances measured in the water-

soluble TPE systems were slightly increased at negative potentials, indicating that the adsorption of the charged TPE derivatives at the water|DCE interface.

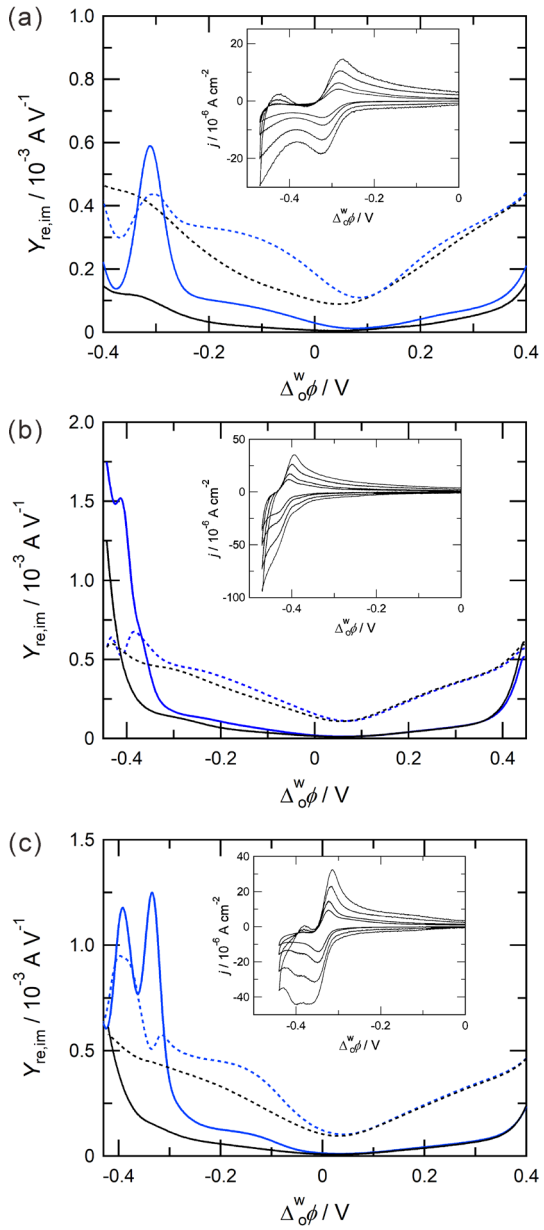

Figure 3. Ac voltammograms measured at the water|DCE interface for **(a)** $TPEDC^{2-}$ at pH 8.8, **(b)** $TPETC^{4-}$ at pH 8.9, and **(c)** $TPETS^{4-}$ at pH 7.0. The solid and dashed lines depict the real (Y_{re}) and imaginary (Y_{im}) components of the admittance, respectively. The blue and black lines refer to the presence and absence of 5.0×10^{-5} mol dm^{-3} TPE derivatives. The ac potential modulation and the linear sweep rate were 10 mV at 7 Hz and 5 mV s^{-1}, respectively. **Insets:** Typical CVs measured at 10, 20, 50, 100 mV s^{-1}.

The PMF data measured for $TPEDC^{2-}$ were shown in **Figure 4a**, in which ΔF_{re} and ΔF_{im} signals maximized around $\Delta_o^w\phi^{o'}_{TPEDC^{2-}}$ were observed with negative and positive signs in agreement with theoretical eqs. for ion transfer responses ($\Delta F_{t,re}$ and $\Delta F_{t,im}$).[39, 50]

$$\Delta F_{t,re} = \frac{4.606\varepsilon\Phi_f I_0}{zFS\cos\psi}\left[\frac{\Delta_o^w\phi_{ac}\sigma\omega^{-3/2}}{(R_{ct}+\sigma\omega^{-1/2})^2+(\sigma\omega^{-1/2})^2}\right] \quad (3)$$

$$\Delta F_{t,im} = -\frac{4.606\varepsilon\Phi_f I_0}{zFS\cos\psi}\left[\frac{\Delta_o^w\phi_{ac}\left(R_{ct}+\sigma\omega^{-1/2}\right)\omega^{-1}}{(R_{ct}+\sigma\omega^{-1/2})^2+(\sigma\omega^{-1/2})^2}\right] \quad (4)$$

where ε is the molar absorption coefficient, Φ_f is the fluorescence quantum yield, I_0 is the intensity of excitation light, F is Faraday constant, and S is the interfacial area. R_{ct} and σ are the charge transfer resistance and the Warburg term, respectively. Eqs.(3) and (4) provide negative $\Delta F_{t,re}$ and positive $\Delta F_{t,im}$ values for $TPEDC^{2-}$ ($z = -2$). On the other hand, the adsorption responses of $TPEDC^{2-}$ with $\Delta F_{a,re} < 0$ and $\Delta F_{a,im} > 0$ were obtained in the wide potential region ($\Delta_o^w\phi^{o'}_{TPEDC^{2-}} < \Delta_o^w\phi < 0.25$ V), indicating a weak potential-dependence of the adsorption process at the aqueous side of the interface (eqs. (5) and (6)).

$$\Delta F_{a,re} = \frac{2.303\varepsilon\Phi I_0\Gamma SzF}{RT}\left[\frac{b\Delta_o^w\phi_{ac}(k^w_{a,dc}\,c_0^w\alpha(1-\theta_{dc})-k^w_{d,dc}(\alpha-1)\theta_{dc})\left(k^w_{a,dc}\,c_0^w+k^w_{d,dc}\right)}{\left(k^w_{a,dc}\,c_0^w+k^w_{d,dc}\right)^2+\omega^2}\right] \quad (5)$$

$$\Delta F_{a,im} = -\frac{2.303\varepsilon\Phi I_0\Gamma SzF}{RT}\left[\frac{b\Delta_o^w\phi_{ac}(k^w_{a,dc}\,c_0^w\alpha(1-\theta_{dc})-k^w_{d,dc}(\alpha-1)\theta_{dc})\omega}{\left(k^w_{a,dc}\,c_0^w+k^w_{d,dc}\right)^2+\omega^2}\right] \quad (6)$$

where Γ, α, c_0^w and θ_{dc} are the saturated interfacial concentration, overall transfer coefficient for adsorption process, the bulk aqueous concentration and the dc surface coverage, respectively. $b\Delta_o^w\phi_{ac}$ is a portion of the Galvani potential difference for the adsorption process. $k^w_{a,dc}$ and $k^w_{d,dc}$ are the dc components of the adsorption and desorption rate constants at given potentials,

respectively. The PMF responses for $TPEDC^{2-}$ seem to those of simple monomeric fluorescent dye but it should be noted that the monomeric TPETC exhibited only a feeble fluorescence in both aqueous and DCE solutions under present alkaline conditions, i.e. AIE-inactive in the bulk phases. Those PMF signals measured in the interfacial region are therefore associated with the interfacial AIE of the adsorbed species. The symmetrically charged $TPETC^{4-}$ and $TPETS^{4-}$ also exhibited significant enhancements of PMF intensities, respectively, at $\Delta_o^w\phi < \Delta_o^w\phi^{o'}_{TPETC^{4-}}$ and $\Delta_o^w\phi < \Delta_o^w\phi^{o'}_{TPETS^{4-}}$ (**Figures 4b** and **4c**), indicating their interfacial AIE features. The PMF results for $TPETS^{4-}$, in particular, indicated apparent interfacial AIE activity maximized around −0.39 V in negative potential sweep, which is more than 60 mV negatively shifted relative to $\Delta_o^w\phi^{o'}_{TPETS^{4-}} = -0.33$ V. The delayed PMF enhancement would result from the aggregation after the accumulation of TPETS monomers at the interface. The TPETS monomer is AIE-inactive in the aqueous phase but it has a small AIE activity in the organic phase, where the emission maximum in DCE ($\varepsilon_{r,DCE} = 10.4$) at 440 nm is located in a short-wavelength region compared to that in water at 466 nm as discussed below. Although the intense emission of TPETS in THF seems to associate with insoluble nanorod or particle formation,[45, 46] the voltammetric data showed the ion transfer features of tetravalent TPETS anions in a quasi-reversible diffusion-limited regime under present conditions (cf. **Figure 3**). The emission observed in the bulk organic phase therefore could arise from a readily dissociable self-aggregate of TPETS without forming a rigid crystalline structure.[46] It is also noteworthy that relatively large PMF intensity in the *s*-polarized light excitation mode was linked to a molecular orientation of fluorescent species at the interface.

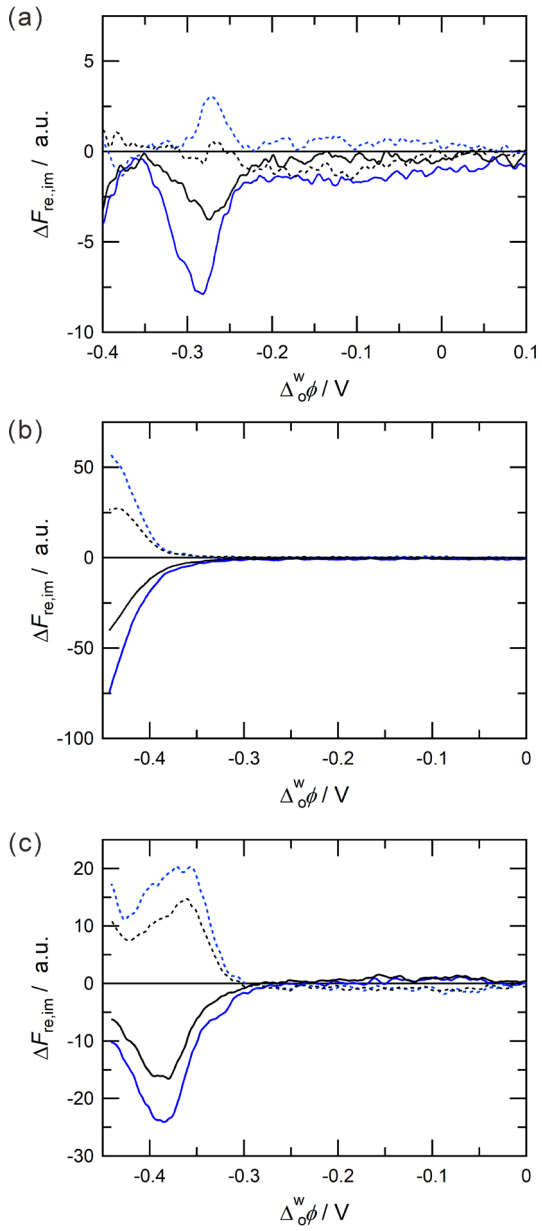

Figure 4. Potential dependences of the PMF responses for **(a)** $TPEDC^{2-}$ at pH 8.8, **(b)** $TPETC^{4-}$ at pH 8.9, and **(c)** $TPETS^{4-}$ at pH 7.0. The solid and dashed lines depict the real (ΔF_{re}) and imaginary (ΔF_{im}) components of PMF, respectively. The blue and black lines refer to PMF measured, respectively, by the *s*- and *p*-polarized excitation beams. The concentration of the TPE derivatives was 5.0×10^{-5} mol dm^{-3}. The ac potential modulation and the linear sweep rate were 20 mV at 1 Hz and 2 mV s^{-1}, respectively.

Characterization of Interfacial Aggregation States. The polarization-modulation fluorescence signals arise only from interfacial species adsorbed with a certain orientation, and undesirable optical signals from randomly oriented bulk species are, in principle, cancel out in the PM-TIRF experiments.[40] The intense PM-TIRF signals with negative sign ($\Delta F^{p\text{-}s} < 0$) were obtained for each TPE derivative (**Figure 5**). The negative $\Delta F^{p\text{-}s}$ signal is indicative of the excitation dipole moment of interfacial species relatively in parallel to the interface in accordance with the PMF results under the *s*-polarized excitation. The PM-TIRF responses showed a significant potential-dependence, where the $\Delta F^{p\text{-}s}$ magnitude was reversibly changed as a function of $\Delta_o^w\phi$ and enhanced around $\Delta_o^w\phi^{o'}$. The potential dependences of $\Delta F^{p\text{-}s}$ for TPETC and TPETS were not synchronized strictly with the voltammetric responses but keep in phase with the delayed PMF responses. As a result, the potential-dependent PM-TIRF responses measured for the interfacial AIE process coincide approximately with the PMF data (cf. **Figure 4**).

The PM-TIRF spectrum considered as emission spectrum of the interfacial species allows us to characterize the adsorption and aggregation states of the interfacial species at given potentials. **Figure 5b** shows the PM-TIRF spectra measured for TPEDC at the interface. As summarized in **Table 1**, TPEDC excited by a cw laser at 376 nm emits only a feeble fluorescence around 478 nm and 441 nm, respectively, in alkaline aqueous and organic phases. The intense PM-TIRF spectra therefore associate with the interfacial aggregates. The PM-TIRF spectra observed prior to the $TPEDC^{2-}$ transfer from water to DCE ($\Delta_o^w\phi \geq -0.19$ V) have an intermediate emission maximum at 462 nm between those of bulk aqueous and organic species. The spectral features of adsorption species often reflect their specific physicochemical properties, and it may result from hydration/solvation state and polarity modified in the interfacial region. TPETC with $\Delta_o^w\phi^{o'}_{TPETC^{4-}} = -0.41$ V indicated similar spectral changes at −0.42 V (**Supporting Information: S4**). In

addition, the PM-TIRF spectra in the TPEDC system indicated apparent red-shift of the emission maximum from 462 nm at $\Delta_o^w\phi \geq -0.19$ V to 482 nm at −0.34 V, indicating a gradual formation of the J-type aggregates at the polarized interface around $\Delta_o^w\phi^{o'}_{TPEDC^{2-}}$.[11, 51] TPETS also showed the red-shift of PM-TIRF spectrum at $\Delta_o^w\phi < \Delta_o^w\phi^{o'}_{TPETS^{4-}}$, in agreement with the J-aggregation after the interfacial accumulation of monomers (**Figure 5c** and **Table 1**). The PM-TIRF analysis demonstrated that the carboxylate and sulfonate derivatives specifically form AIE-active J-aggregates in the interfacial region by applying appropriate potentials.

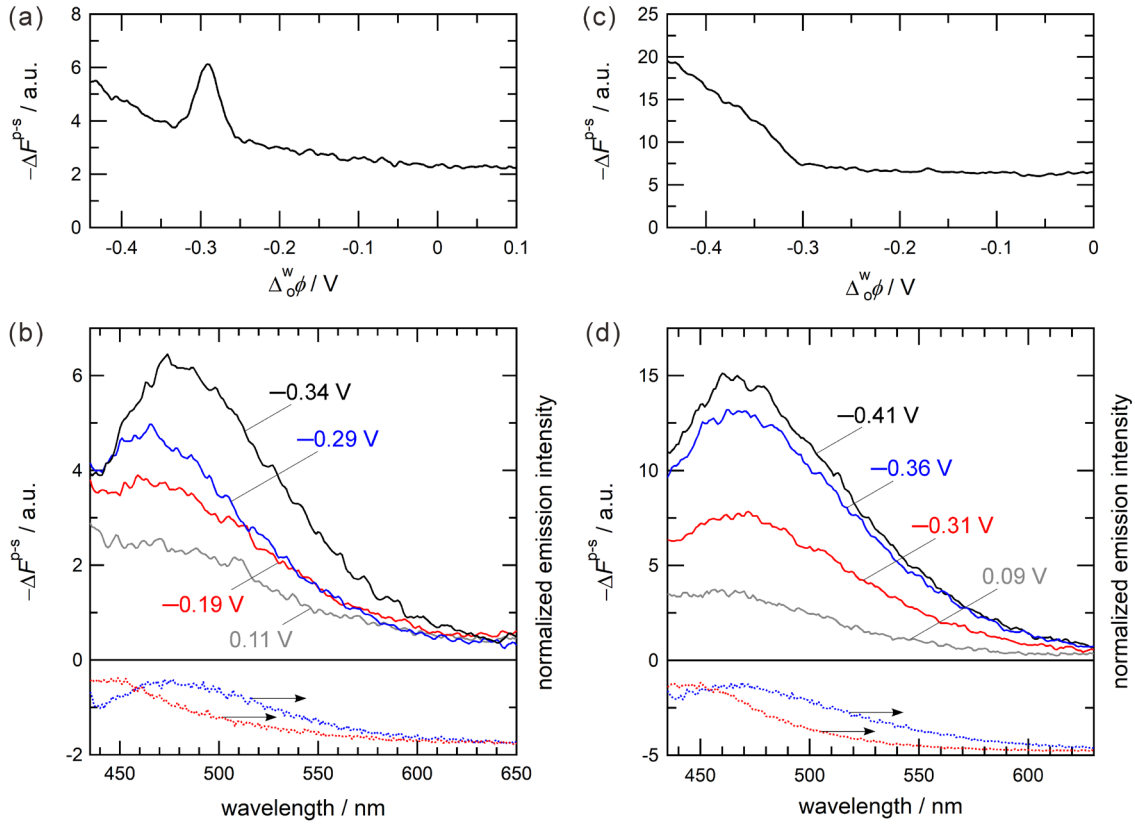

Figure 5. Potential dependences of PM-TIRF intensity at 460 nm and PM-TIRF spectra for **(a,b)** $TPEDC^{2-}$ and **(c,d)** $TPETS^{4-}$ at the water|DCE interface. The dotted lines refer to the normalized emission spectra measured in the aqueous (blue) and organic (red) phases. The concentrations of the TPE derivatives was 5.0×10^{-5} mol dm^{-3} in the aqueous phase (pH 9.0 for $TPEDC^{2-}$ and pH 7.1 for $TPETS^{4-}$). **(a,c)** The potential sweep rate was 2 mV s^{-1} in negative sweep.

Table 1. Emission maxima of TPE derivatives at the water|DCE interface and in solutions[a]

	TPEDC system		TPETC system		TPETS system	
	$\Delta_o^w\phi$ / V	$\lambda_{em,max}$ / nm	$\Delta_o^w\phi$ / V	$\lambda_{em,max}$ / nm	$\Delta_o^w\phi$ / V	$\lambda_{em,max}$ / nm
interface (PM-TIRF)	0.11	462	0.10	461	0.09	455
	−0.19	462	−0.35	458	−0.31	467
	−0.29	465	−0.42	464	−0.36	469
	−0.34	482	−0.47	466	−0.41	469
aqueous phase	(pH 9.0)	478	(pH 9.0)	469	(pH 7.1)	466
organic phase		441		453		440

[a] The emission maximum wavelengths ($\lambda_{em,max}$) were measured with a cw laser at 376 nm.

AIE Behavior at Biomimetic Interfaces. The potential-induced interfacial AIE reaction found in the present study suggests the potential ability of simple water-soluble TPE derivatives to visualize the dynamic polarization of biomembranes or organic tissues. The DMPC-adsorbed water|DCE interface was employed for evaluating the AIE activity of anionic TPEs on a biomembrane surface. In all the examined systems, typical voltammetric features for phospholipid-adsorbed interfaces were observed, in which the capacitive current was reduced by the interfacial adsorption of neutral DMPC molecules and the facilitated lithium ion transfer appeared close to the positive edge of the potential window (0.2 V < $\Delta_o^w\phi$) (**Supporting Information: S5**).[52-54] The ion transfer responses of $TPEDC^{2-}$ at $\Delta_o^w\phi^{\circ'}_{TPEDC^{2-}}$ were hardly affected by the DMPC layer but PM-TIRF results clarified the specific interaction between TPEDC and DMPC at the interface. As shown in **Figure 6**, the maximum intensity of negative $\Delta F^{p\text{-}s}$ signals was observed around −0.35 V, which is 50 mV more negative potential than $\Delta_o^w\phi^{\circ'}_{TPEDC^{2-}}$ at the bare water|DCE interface. The voltammetric and PM-TIRF results demonstrate that the potential-dependence of the interfacial AIE process of TPEDC is modified on the DMPC layer even though $\Delta_o^w\phi^{\circ'}_{TPEDC^{2-}}$ associated with the Gibbs energy of

transfer between water and DCE (i.e. $\Delta G^{w\to o}_{tr.TPEDC^{2-}} = -2F\Delta^{w}_{o}\phi^{o'}_{TPEDC^{2-}}$) remained unchanged in the presence of DMPC. The emission maximum of the PM-TIRF spectrum at −0.34 V was measured at 470 nm, which is the intermediate value between the aqueous and organic phases, suggesting that the AIE mechanism of $TPEDC^{2-}$ observed at the bare interface is effectively modified on the membrane surface (**Table 2**). In addition, no AIE was observed in the bulk organic phase including free DMPC monomers. The intense emission from the interfacial region in the biomimetic system could be associated with the direct RIM mechanism of TPEDC in the DMPC layer.[11, 12]

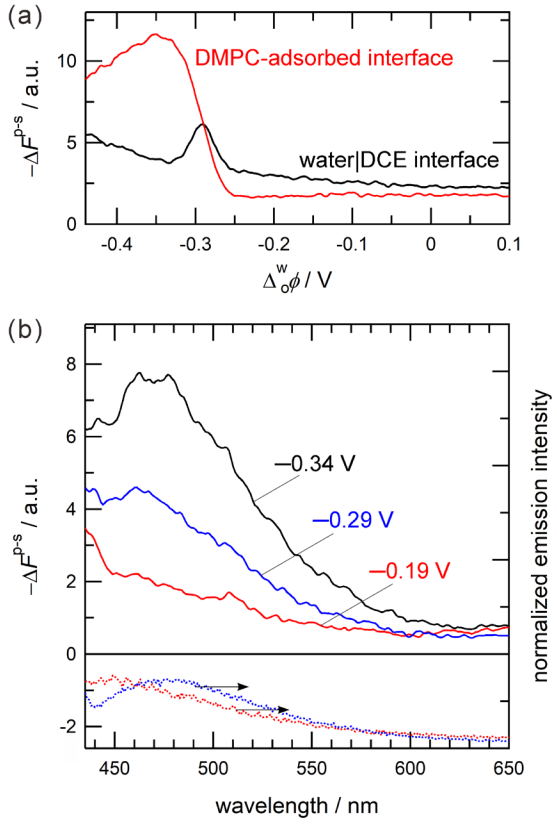

Figure 6. Potential dependences of **(a)** PM-TIRF intensity at 460 nm and **(b)** PM-TIRF spectra for $TPEDC^{2-}$ at the DMPC-adsorbed interface. The dotted lines refer to the normalized emission spectra measured in the aqueous (blue) and organic (red) phases. The concentrations of TPEDC and DMPC were 5.0×10^{-5} mol dm^{-3} in the aqueous phase (pH 9.0) and 2.0×10^{-5} mol dm^{-3} in the organic phase, respectively. **(a)** The potential sweep rate was 2 mV s^{-1} in negative sweep.

Table 2. Emission maxima of TPE derivatives at the DMPC-adsorbed interface and in solutions [a]

	TPEDC system		TPETC system		TPETS system	
	$\Delta_o^w\phi$ / V	$\lambda_{em,max}$ / nm	$\Delta_o^w\phi$ / V	$\lambda_{em,max}$ / nm	$\Delta_o^w\phi$ / V	$\lambda_{em,max}$ / nm
interface (PM-TIRF)					0.09	473
	−0.19	−	−0.35	464	−0.31	475
	−0.29	460	−0.42	479	−0.36	484
	−0.34	470	−0.47	479	−0.41	484
aqueous phase	(pH 9.0)	478	(pH 9.0)	469	(pH 7.1)	466
organic phase		441		457		468

[a] The emission maximum wavelengths ($\lambda_{em,max}$) were measured with a cw laser at 376 nm.

In the symmetrically charged $TPETC^{4-}$ and $TPETS^{4-}$ systems, the ion transfer responses in ac voltammograms were weakened and negatively shifted at the biomimetic interface (**Supporting Information: S5**). The slow kinetic process across the DMPC layer could be responsible for the small voltammetric responses. On the other hand, the large red-shift of emission maxima in the PM-TIRF spectrum is associated with the promotion of J-aggregation on the DMPC layer (**Figure 7** and **Table 2**). In addition, the emission spectrum of TPETS measured in the organic phase containing free DMPC molecules showed a weak emission with a 15 nm red-shifted maximum at 468 nm, indicating the effective interaction between the TPETS anions and DMPC in the bulk organic phase. These results indicate that the DMPC layer stimulates the interfacial AIE process of tetra-anionic TPEs, in which the interaction with DMPC was more effective for TPETS.

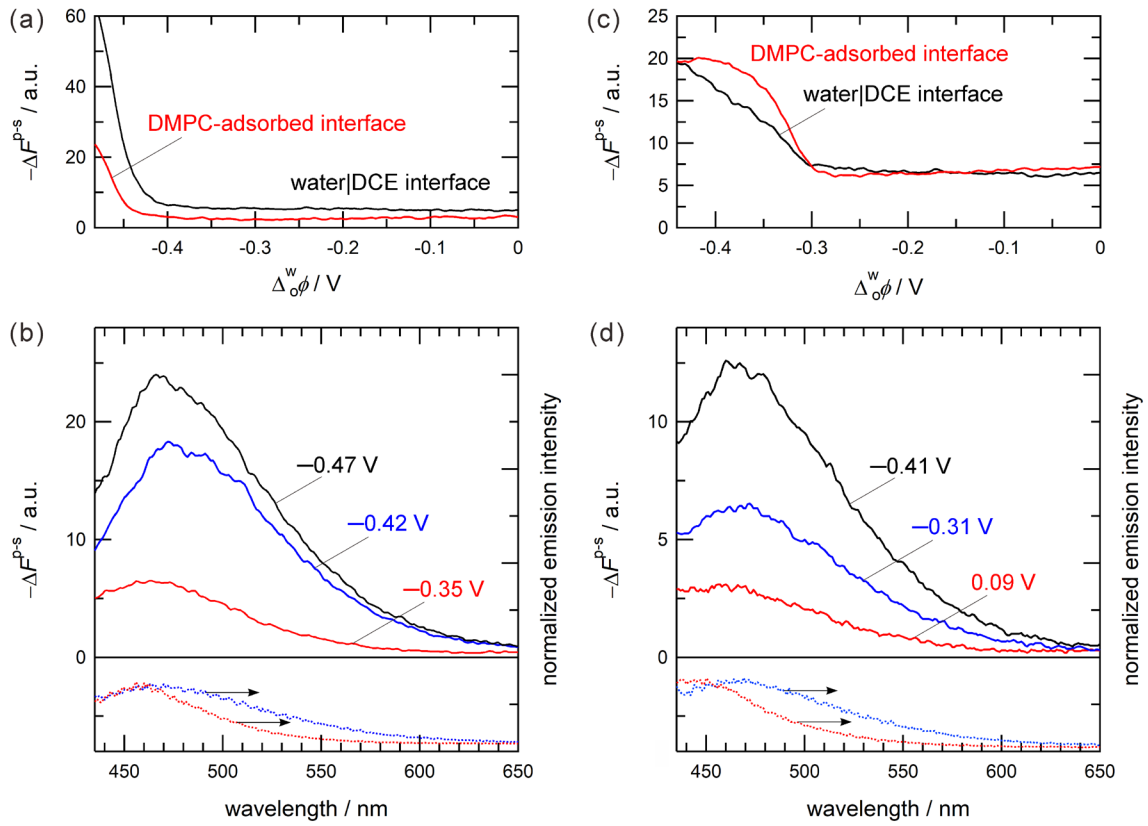

Figure 7. Potential dependences of PM-TIRF intensity at 460 nm and PM-TIRF spectra for **(a,b)** $TPETC^{4-}$ and **(c,d)** $TPETS^{4-}$ at the DMPC-adsorbed interface. The dotted lines refer to the normalized emission spectra measured in the aqueous (blue) and organic (red) phases. The concentrations of the TPE derivatives and DMPC were 5.0×10^{-5} mol dm^{-3} in the aqueous phase (pH 9.0 for $TPETC^{4-}$ and pH 7.0 for $TPETS^{4-}$) and 2.0×10^{-5} mol dm^{-3} in the organic phase, respectively. **(a,c)** The potential sweep rate was 2 mV s^{-1} in negative sweep.

Conclusions

The interfacial AIE behavior of the anionic TPE derivatives examined in this study was reversibly modulated depending on the externally applied potential. The anionic carboxylate derivatives, $TPEDC^{2-}$ and $TPETC^{4-}$, exhibited the interface-sensitive AIE feature but no emission from the bulk aqueous and organic phases. On the other hand, $TPETS^{4-}$ formed the aggregates with distinguishable emission properties at the interface and in the organic solution. Those specific AIE

responses show the advantage of the TPE-based AIEgens for sensitive-imaging of liquid interfaces and surfaces of micelles and polymers often buried in optical responses arising from bulk solution phases. The potential-induced AIE behavior observed for simple water-soluble TPE derivatives at the phospholipid-adsorbed interface is also important to develop the membrane-potential sensitive probe in biomedical applications, especially, noncovalent labeling of liposomes and exosomes.

Corresponding Author

Hirohisa Nagatani

E-mail: nagatani@se.kanazawa-u.ac.jp

ORCID: 0000-0001-8678-5715

Supporting Information.

^{1}H NMR data for TPETS, UV-vis absorption and emission spectra in aqueous solutions, AIE responses in THF-water mixtures, PM-TIRF data for TPETC, ac voltammograms at biomimetic interfaces.

ACKNOWLEDGMENTS

This work was supported by a Grant-in-Aid for Scientific Research (C) (no. 19K05541) from Japan Society for the Promotion of Science (JSPS) and the Shibuya Foundation for Science, Culture and Sports. We thank Emer. Prof. Hisanori Imura of Kanazawa University for valuable discussions.

REFERENCES

(1) Mei, J.; Leung, N. L.; Kwok, R. T.; Lam, J. W.; Tang, B. Z., Aggregation-Induced Emission: Together We Shine, United We Soar! *Chem. Rev.* **2015,** *115*, 11718-940.

(2) Zong, L.; Xie, Y.; Wang, C.; Li, J. R.; Li, Q.; Li, Z., From ACQ to AIE: the suppression of the strong π-π interaction of naphthalene diimide derivatives through the adjustment of their flexible chains. *Chem. Commun.* **2016,** *52*, 11496-11499.

(3) Klymchenko, A. S., Solvatochromic and Fluorogenic Dyes as Environment-Sensitive Probes: Design and Biological Applications. *Acc. Chem. Res.* **2017,** *50*, 366-375.

(4) Feng, H. T.; Lam, J. W. Y.; Tang, B. Z., Self-assembly of AIEgens. *Coord. Chem. Rev.* **2020,** *406*.

(5) Hong, Y.; Lam, J. W.; Tang, B. Z., Aggregation-Induced Emission. *Chem. Soc. Rev.* **2011,** *40*, 5361-88.

(6) Wang, H.; Liu, G., Advances in Luminescent Materials with Aggregation-Induced Emission (AIE) Properties for Biomedical Applications. *J. Mater. Chem. B* **2018,** *6*, 4029-4042.

(7) Zhu, C.; Kwok, R. T. K.; Lam, J. W. Y.; Tang, B. Z., Aggregation-Induced Emission: A Trailblazing Journey to the Field of Biomedicine. *ACS Appl. Bio Mater.* **2018,** *1*, 1768-1786.

(8) Hong, Y.; Lam, J. W.; Tang, B. Z., Aggregation-Induced Emission: Phenomenon, Mechanism and Applications. *Chem. Commun.* **2009**, 4332-53.

(9) Zhao, Z.; He, B.; Tang, B. Z., Aggregation-Induced Emission of Siloles. *Chem. Sci.* **2015,** *6*, 5347-5365.

(10) Li, Q.; Li, Z., The Strong Light-Emission Materials in the Aggregated State: What Happens from a Single Molecule to the Collective Group. *Adv. Sci.* **2017,** *4*.

(11) Crespo-Otero, R.; Li, Q.; Blancafort, L., Exploring Potential Energy Surfaces for Aggregation-Induced Emission-From Solution to Crystal. *Chem Asian J* **2019,** *14*, 700-714.

(12) Leung, N. L.; Xie, N.; Yuan, W.; Liu, Y.; Wu, Q.; Peng, Q.; Miao, Q.; Lam, J. W.; Tang, B. Z., Restriction of Intramolecular Motions: The General Mechanism behind Aggregation-Induced Emission. *Chem. Eur. J* **2014,** *20*, 15349-53.

(13) Booth, S. G.; Dryfe, R. A. W., Assembly of Nanoscale Objects at the Liquid/Liquid Interface. *J. Phys. Chem. C* **2015,** *119*, 23295-23309.

(14) Toor, A.; Feng, T.; Russell, T. P., Self-Assembly of Nanomaterials at Fluid Interfaces. *Eur. Phys. J. E* **2016,** *39*.

(15) Shrestha, L. K.; Hill, J. P.; Tsuruoka, T.; Miyazawa, K.; Ariga, K., Surfactant-Assisted Assembly of Fullerene (C_{60}) Nanorods and Nanotubes Formed at a Liquid-Liquid Interface. *Langmuir* **2013,** *29*, 7195-7202.

(16) Nuraje, N.; Su, K.; Yang, N. I.; Matsui, H., Liquid/Liquid Interfacial Polymerization to Grow Single Crystalline Nanoneedles of Various Conducting Polymers. *ACS Nano* **2008,** *2*, 502-506.

(17) Volkov, A. G., *Liquid Interfaces in Chemical, Biological, and Pharmaceutical Applications*. Marcel Dekker: New York, 2001.

(18) Osakai, T., Is the Oil|Water Interface the Simplest and Best Suited Model for Understanding Biomembranes? *Anal. Sci.* **2019,** *35*, 361-366.

(19) Santos, H. A.; García-Morales, V.; Pereira, C. M., Electrochemical Properties of Phospholipid Monolayers at Liquid-Liquid Interfaces. *ChemPhysChem* **2010,** *11*, 28-41.

(20) Yamamoto, S.; Nagatani, H.; Imura, H., Potential-Induced Aggregation of Anionic Porphyrins at Liquid|Liquid Interfaces. *Langmuir* **2017,** *33*, 10134-10142.

(21) Nagatani, H.; Samec, Z.; Brevet, P.-F.; Fermín, D. J.; Girault, H. H., Adsorption and Aggregation of *meso*-Tetrakis(4-carboxyphenyl)porphyrinato Zinc(II) at the Polarized Water|1,2-Dichloroethane Interface. *J. Phys. Chem. B* **2003,** *107*, 786-790.

(22) Scanlon, M. D.; Smirnov, E.; Stockmann, T. J.; Peljo, P., Gold Nanofilms at Liquid-Liquid Interfaces: An Emerging Platform for Redox Electrocatalysis, Nanoplasmonic Sensors, and Electrovariable Optics. *Chem. Rev.* **2018,** *118*, 3722-3751.

(23) Abid, J. P.; Abid, M.; Bauer, C.; Girault, H. H.; Brevet, P.-F., Controlled Reversible Adsorption of Core-Shell Metallic Nanoparticles at the Polarized Water/1,2-Dichloroethane Interface Investigated by Optical Second-Harmonic Generation. *J. Phys. Chem. C* **2007,** *111*, 8849-8855.

(24) Su, B.; Abid, J. P.; Fermín, D. J.; Girault, H. H.; Hoffmannová, H.; Krtil, P.; Samec, Z., Reversible Voltage-Induced Assembly of Au Nanoparticles at Liquid|Liquid Interfaces. *J. Am. Chem. Soc.* **2004,** *126*, 915-919.

(25) Fluhler, E.; Burnham, V. G.; Loew, L. M., Spectra, Membrane Binding, and Potentiometric Reponses of New Charge Shift Probes. *Biochem.* **1985,** *24*, 5749-5755.

(26) Loew, L. M., Potentiometric Dyes: Imaging Electrical Activity of Cell Membranes. *Pure Appl. Chem.* **1996,** *68*, 1405-1409.

(27) Baxter, D. F.; Kirk, M.; Garcia, A. F.; Raimondi, A.; Holmqvist, M. H.; Flint, K. K.; Bojanic, D.; Distefano, P. S.; Curtis, R.; Xie, Y., A Novel Membrane Potential-Sensitive Fluorescent Dye Improves Cell-Based Assays for Ion Channels. *J. Biomol. Screening* **2002,** *7*, 79-85.

(28) Miller, E. W.; Lin, J. Y.; Frady, E. P.; Steinbach, P. A.; Kristan Jr, W. B.; Tsien, R. Y., Optically Monitoring Voltage in Neurons by Photoinduced Electron Transfer Through Molecular Wires. *Proc. Natl. Acad. Sci. U. S. A.* **2012,** *109*, 2114-2119.

(29) Woodford, C. R.; Frady, E. P.; Smith, R. S.; Morey, B.; Canzi, G.; Palida, S. F.; Araneda, R. C.; Kristan, W. B.; Kubiak, C. P.; Miller, E. W.; Tsien, R. Y., Improved PeT Molecules for Optically Sensing Voltage in Neurons. *J. Am. Chem. Soc.* **2015,** *137*, 1817-1824.

(30) Li, L. S., Fluorescence Probes for Membrane Potentials Based on Mesoscopic Electron Transfer. *Nano Lett.* **2007,** *7*, 2981-2986.

(31) Li, J.; Kwon, N.; Jeong, Y.; Lee, S.; Kim, G.; Yoon, J., Aggregation-Induced Fluorescence Probe for Monitoring Membrane Potential Changes in Mitochondria. *ACS Appl. Mater. Interfaces* **2018,** *10*, 12150-12154.

(32) Leung, C. W. T.; Hong, Y.; Chen, S.; Zhao, E.; Lam, J. W. Y.; Tang, B. Z., A Photostable AIE Luminogen for Specific Mitochondrial Imaging and Tracking. *J. Am. Chem. Soc.* **2013,** *135*, 62-65.

(33) Hu, Q.; Gao, M.; Feng, G.; Liu, B., Mitochondria-Targeted Cancer Therapy Using a Light-Up Probe with Aggregation-Induced-Emission Characteristics. *Angew. Chem., Int. Ed.* **2014,** *53*, 14225-14229.

(34) Zhao, N.; Chen, S.; Hong, Y.; Tang, B. Z., A Red Emitting Mitochondria-Targeted AIE Probe As an Indicator for Membrane Potential and Mouse Sperm Activity. *Chem. Commun.* **2015,** *51*, 13599-602.

(35) Gui, C.; Zhao, E.; Kwok, R. T. K.; Leung, A. C. S.; Lam, J. W. Y.; Jiang, M.; Deng, H.; Cai, Y.; Zhang, W.; Su, H.; Tang, B. Z., AIE-active theranostic system: selective staining and killing of cancer cells. *Chem. Sci.* **2017,** *8*, 1822-1830.

(36) Ma, X.; Zhang, J.; Zhang, Y.; Liu, J., Adsorption Promoted Aggregation-Induced Emission Showing Strong Dye Lateral Interactions. *Langmuir* **2019,** *35*, 16304-16311.

(37) Zhang, H.; Sun, J. Z.; Liu, J.; Kwok, R. T. K.; Lam, J. W. Y.; Tang, B. Z., Visualizing and Monitoring Interface Structures and Dynamics by Luminogens with Aggregation-Induced Emission. *J. Appl. Phys.* **2019,** *126*, 050901.

(38) Li, J.; Li, Y.; Chan, C. Y. K.; Kwok, R. T. K.; Li, H.; Zrazhevskiy, P.; Gao, X.; Sun, J. Z.; Qin, A.; Tang, B. Z., An Aggregation-Induced-Emission Platform for Direct Visualization of Interfacial Dynamic Self-Assembly. *Angew Chem Int Ed Engl* **2014,** *53*, 13518-13522.

(39) Nagatani, H.; Fermín, D. J.; Girault, H. H., A Kinetic Model for Adsorption and Transfer of Ionic Species at Polarized Liquid|Liquid Interfaces as Studied by Potential Modulated Fluorescence Spectroscopy. *J. Phys. Chem. B* **2001,** *105*, 9463-9473.

(40) Yamamoto, S.; Nagatani, H.; Morita, K.; Imura, H., Potential-Dependent Adsorption and Orientation of *meso*-Substituted Porphyrins at Liquid|Liquid Interfaces Studied by Polarization-Modulation Total Internal Reflection Fluorescence Spectroscopy. *J. Phys. Chem. C* **2016,** *120*, 7248-7255.

(41) Yamamoto, S.; Kanai, S.; Takeyama, M.; Nishiyama, Y.; Imura, H.; Nagatani, H., Ion Transfer and Adsorption of Water-Soluble Metal Complexes of 8-Hydroxyquinoline Derivatives at the Water|1,2-Dichloroethane Interface. *J. Electroanal. Chem.* **2020,** *856*, 113566.

(42) Kakiuchi, T.; Takasu, Y., Differential Cyclic Voltfluorometry and Chronofluorometry of the Transfer of Fluorescent Ions across the 1,2-Dichloroethane-Water Interface. *Anal. Chem.* **1994,** *66*, 1853-1859.

(43) Ding, Z.; Wellington, R. G.; Brevet, P. F.; Girault, H. H., Spectroelectrochemical Studies of $Ru(bpy)_3^{2+}$ at the Water/1,2-Dichloroethane Interface. *J. Phys. Chem.* **1996,** *100*, 10658-10663.

(44) Nagatani, H.; Suzuki, S.; Fermín, D. J.; Girault, H. H.; Nakatani, K., Interfacial Behavior of Sulforhodamine 101 at the Polarized Water/1,2-Dichloroethane Interface Studied by Spectroelectrochemical Techniques. *Anal. Bioanal. Chem.* **2006,** *386*, 633-638.

(45) Ooyama, Y.; Sugino, M.; Enoki, T.; Yamamoto, K.; Tsunoji, N.; Ohshita, J., Aggregation-Induced Emission (AIE) Characteristic of Water-Soluble Tetraphenylethene (TPE) Bearing Four Sulfonate Salts. *New J. Chem.* **2017,** *41*, 4747-4749.

(46) La, D. D.; Anuradha, A.; Hundal, A. K.; Bhosale, S. V.; Jones, L. A.; Bhosale, S. V., pH-Dependent Self-Assembly of Water-Soluble Sulfonate-Tetraphenylethylene with Aggregation-Induced Emission. *Supramol. Chem.* **2017,** *30*, 1-8.

(47) Nagatani, H.; Sagara, T., Potential-Modulation Spectroscopy at Solid/Liquid and Liquid/Liquid Interfaces. *Anal. Sci.* **2007,** *23*, 1041-1048.

(48) Wandlowski, T.; Marecek, V.; Samec, Z., Galvani Potential Scales for Water-Nitrobenzene and Water-1,2-Dichloroethane Interfaces. *Electrochim. Acta* **1990,** *35*, 1173-1175.

(49) Crutchfield, F. E.; Gibson, J. A.; Hall, J. L., Dielectric Constant and Refractive Index from 20 to 35° and Density at 25° for the System Tetrahydrofuran-Water. *J. Am. Chem. Soc.* **1953,** *75*, 6044-6045.

(50) Nagatani, H.; Sagara, T., Potential-modulation spectroscopy at solid/liquid and liquid/liquid interfaces. *Anal. Sci.* **2007,** *23*, 1041-1048.

(51) Hestand, N. J.; Spano, F. C., Expanded Theory of H- and J-Molecular Aggregates: The Effects of Vibronic Coupling and Intermolecular Charge Transfer. *Chem Rev* **2018,** *118*, 7069-7163.

(52) Samec, Z.; Trojánek, A.; Girault, H. H., Thermodynamic Analysis of the Cation Binding to a Phosphatidylcholine Monolayer at a Polarised Interface Between Two Immiscible Electrolyte Solutions. *Electrochem. Commun.* **2003,** *5*, 98-103.

(53) Yoshida, Y.; Maeda, K.; Shirai, O., The Complex Formation of Ions with a Phospholipid Monolayer Adsorbed at an Aqueous|1,2-Dichloroethane Interface. *J. Electroanal. Chem.* **2005,** *578*, 17-24.

(54) Manzanares, J. A.; Allen, R. M.; Kontturi, K., Enhanced Ion Transfer Rate Due to the Presence of Zwitterionic Phospholipid Monolayers at the ITIES. *J. Electroanal. Chem.* **2000,** *483*, 188-196.

Table of Contents Image

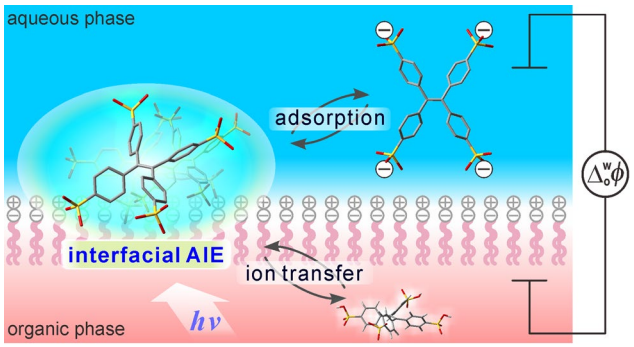

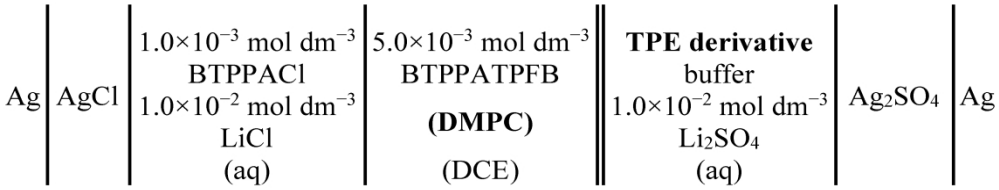

Figure 1. Composition of the electrochemical cell.

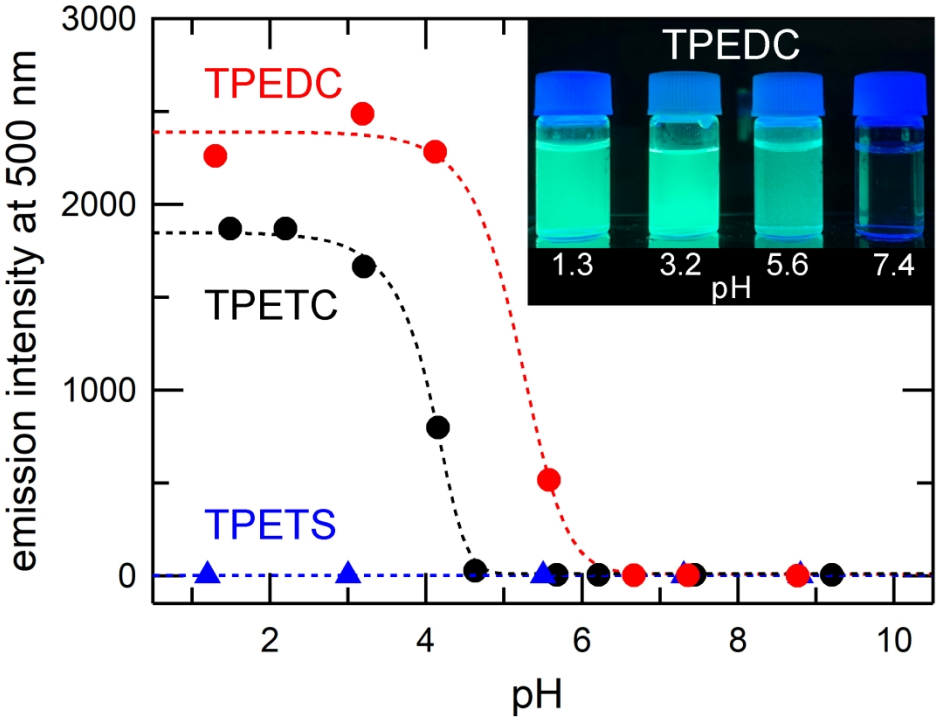

Figure 2. pH dependences of the emission intensity at 500 nm of TPE derivatives in aqueous solution. The red, black, and blue symbols depict TPEDC, TPETC, and TPETS, respectively. The excitation wavelength was 376 nm and the concentration of the TPE derivatives was 2.0×10^{-5} mol dm^{-3}. Inset: Typical fluorescence image of TPEDC in aqueous solution under UV irradiation (365 nm).

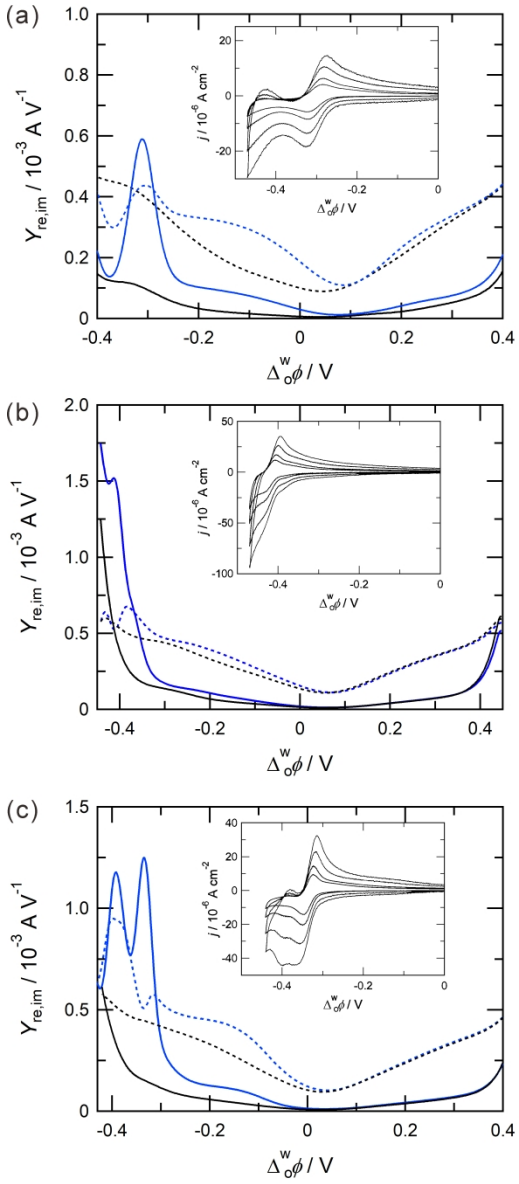

Figure 3. Ac voltammograms measured at the water|DCE interface for (a) $TPEDC^{2-}$ at pH 8.8, (b) $TPETC^{4-}$ at pH 8.9, and (c) $TPETS^{4-}$ at pH 7.0. The solid and dashed lines depict the real (Y_{re}) and imaginary (Y_{im}) components of the admittance, respectively. The blue and black lines refer to the presence and absence of 5.0×10^{-5} mol dm^{-3} TPE derivatives. The ac potential modulation and the linear sweep rate were 10 mV at 7 Hz and 5 mV s−1, respectively. Insets: Typical CVs measured at 10, 20, 50, 100 mV s^{-1}.

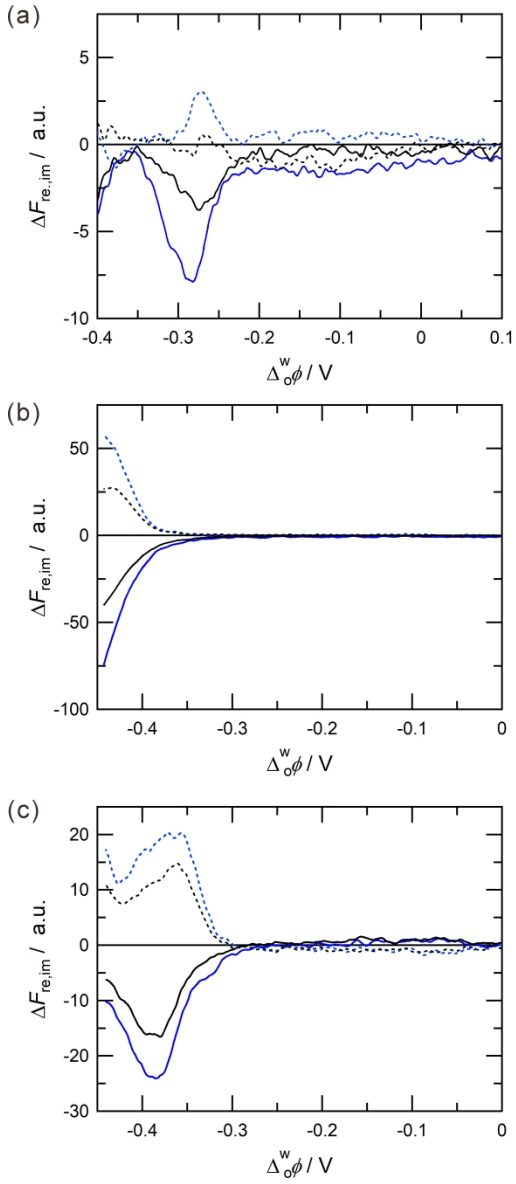

Figure 4. Potential dependences of the PMF responses for (a) $TPEDC^{2-}$ at pH 8.8, (b) $TPETC^{4-}$ at pH 8.9, and (c) $TPETS^{4-}$ at pH 7.0. The solid and dashed lines depict the real (ΔF_{re}) and imaginary (ΔF_{im}) components of PMF, respectively. The blue and black lines refer to PMF measured, respectively, by the s- and p-polarized excitation beams. The concentration of the TPE derivatives was 5.0×10^{-5} mol dm^{-3}. The ac potential modulation and the linear sweep rate were 20 mV at 1 Hz and 2 mV s^{-1}, respectively.

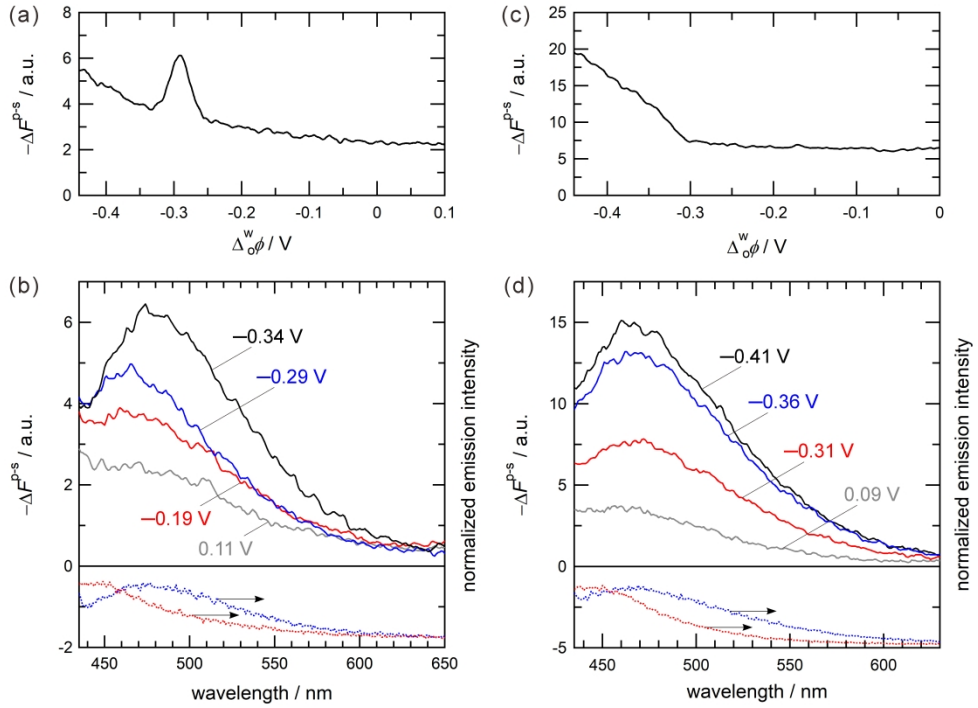

Figure 5. Potential dependences of PM-TIRF intensity at 460 nm and PM-TIRF spectra for (a,b) $TPEDC^{2-}$ and (c,d) $TPETS^{4-}$ at the water|DCE interface. The dotted lines refer to the normalized emission spectra measured in the aqueous (blue) and organic (red) phases. The concentrations of the TPE derivatives was 5.0×10^{-5} mol dm^{-3} in the aqueous phase (pH 9.0 for $TPEDC^{2-}$ and pH 7.1 for $TPETS^{4-}$). (a,c) The potential sweep rate was 2 mV s^{-1} in negative sweep.

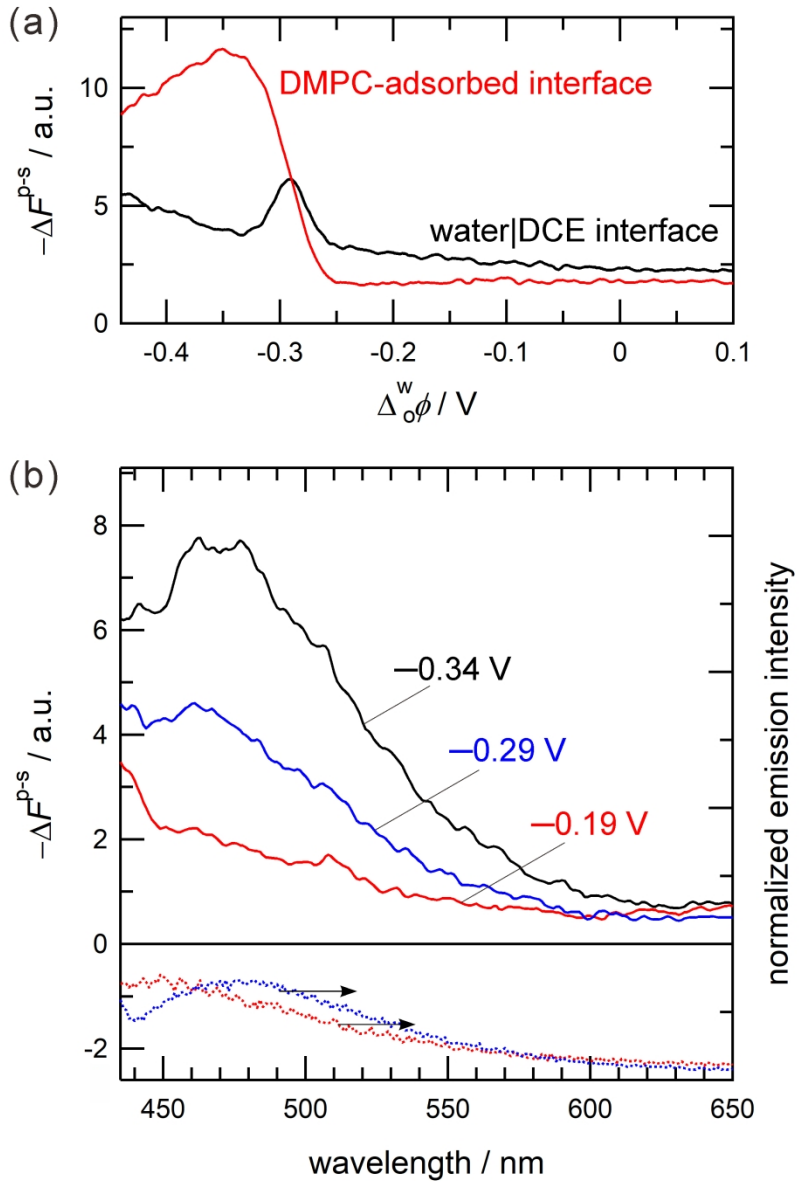

Figure 6. Potential dependences of (a) PM-TIRF intensity at 460 nm and (b) PM-TIRF spectra for $TPEDC^{2-}$ at the DMPC-adsorbed interface. The dotted lines refer to the normalized emission spectra measured in the aqueous (blue) and organic (red) phases. The concentrations of TPEDC and DMPC were 5.0×10^{-5} mol dm^{-3} in the aqueous phase (pH 9.0) and 2.0×10^{-5} mol dm^{-3} in the organic phase, respectively. (a) The potential sweep rate was 2 mV s^{-1} in negative sweep.

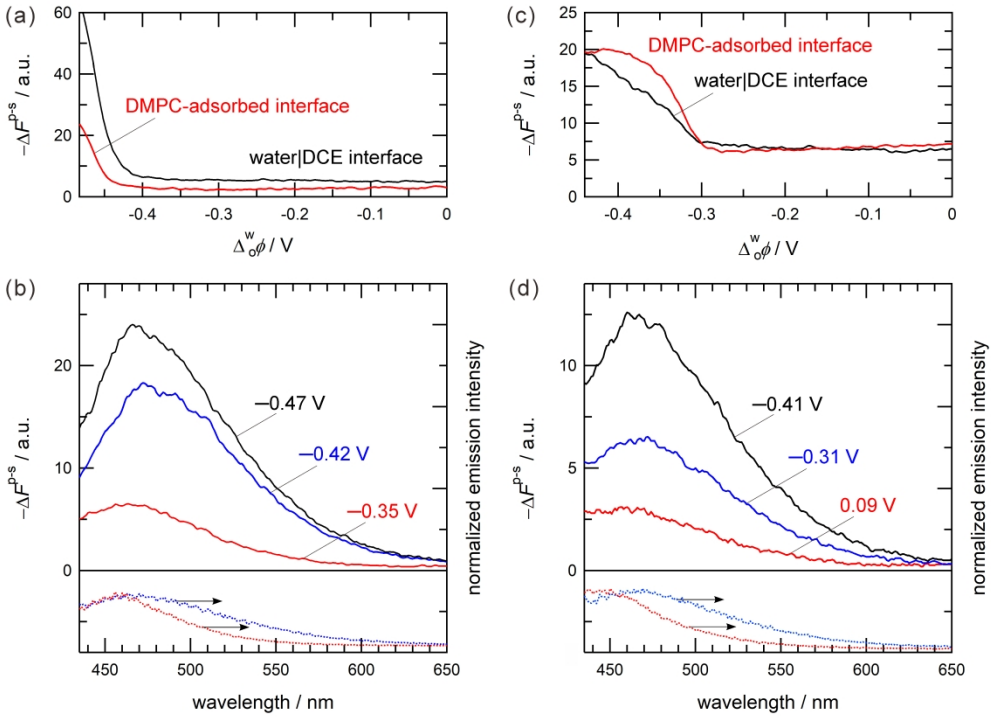

Figure 7. Potential dependences of PM-TIRF intensity at 460 nm and PM-TIRF spectra for (a,b) $TPETC^{4-}$ and (c,d) $TPETS^{4-}$ at the DMPC-adsorbed interface. The dotted lines refer to the normalized emission spectra measured in the aqueous (blue) and organic (red) phases. The concentrations of the TPE derivatives and DMPC were 5.0×10^{-5} mol dm^{-3} in the aqueous phase (pH 9.0 for $TPETC^{4-}$ and pH 7.0 for $TPETS^{4-}$) and 2.0×10^{-5} mol dm^{-3} in the organic phase, respectively. (a,c) The potential sweep rate was 2 mV s^{-1} in negative sweep.

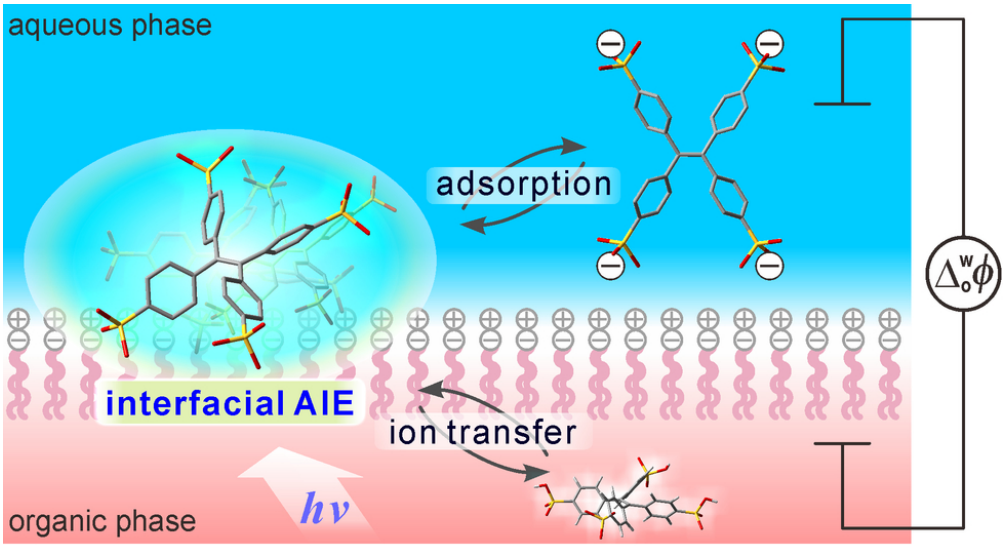

Table of Contents Image

82x45mm (300 x 300 DPI)